

Monte Carlo approach for hadron azimuthal correlations in high energy proton and nuclear collisions

Alejandro Ayala¹, Isabel Dominguez¹, Jamal Jalilian-Marian², J. Magnin³ and Maria Elena Tejeda-Yeomans⁴

¹*Instituto de Ciencias Nucleares, Universidad Nacional Autónoma de México,
Apartado Postal 70-543, México Distrito Federal 04510, Mexico.*

²*Department of Natural Sciences, Baruch College, New York,
New York 10010, USA and CUNY Graduate Center,
365 Fifth Avenue, New York, New York 10016, USA.*

³*Centro Brasileiro de Pesquisas Físicas, CBPF, Rua Dr. Xavier Sigaud 150, 22290-180, Rio de Janeiro, Brazil.*

⁴*Departamento de Física, Universidad de Sonora, Boulevard Luis Encinas J. y Rosales,
Colonia Centro, Hermosillo, Sonora 83000, Mexico.*

We use a Monte Carlo approach to study hadron azimuthal angular correlations in high energy proton-proton and central nucleus-nucleus collisions at the BNL Relativistic Heavy Ion Collider (RHIC) energies at mid-rapidity. We build a hadron event generator that incorporates the production of $2 \rightarrow 2$ and $2 \rightarrow 3$ parton processes and their evolution into hadron states. For nucleus-nucleus collisions we include the effect of parton energy loss in the Quark-Gluon Plasma using a modified fragmentation function approach. In the presence of the medium, for the case when three partons are produced in the hard scattering, we analyze the Monte Carlo sample in parton and hadron momentum bins to reconstruct the angular correlations. We characterize this sample by the number of partons that are able to hadronize by fragmentation within the selected bins. In the nuclear environment the model allows hadronization by fragmentation only for partons with momentum above a threshold $p_T^{\text{thresh}} = 2.4$ GeV. We argue that one should treat properly the effect of those partons with momentum below the threshold, since their interaction with the medium may lead to showers of low momentum hadrons along the direction of motion of the original partons as the medium becomes diluted.

PACS numbers: 25.75.-q, 25.75.Gz, 12.38.Bx

I. INTRODUCTION

One of the main experimental discoveries in the field of high energy heavy-ion reactions has been the suppression of particles, with momentum similar to the leading one, in the away side of azimuthal angular correlations [1]. It is by now believed that this phenomenon is caused by the energy loss of partons moving through the strongly interacting medium formed in the aftermath of the reaction. This picture is far from being that simple since when the difference in momentum between leading and away side particles increases, either a double peak structure or a broadening of the away-side peak appears, while either of these are absent in $p + p$ collisions at the same energies [2].

Given that the structures in the away side are more prominent for relatively small momentum particles, the above features have generated different explanations based on medium effects. The current trend explains the double peak/broadening in the away side as due to initial state fluctuations of the matter density in the colliding nuclei. These fluctuations would in turn be responsible for an anisotropic flow of partially equilibrated low momentum particles with the bulk medium. Recent descriptions of this scenario, based on hydrodynamics, have reproduced successfully the experimental v_3 [3]. Nonetheless, it has also been shown recently that there is a strong connection between the medium's path length and the observed away side structures [4]. This connection is ex-

pressed through the dependence of the azimuthal correlation on the trigger particle direction with respect to the event plane in such a way that, for selected trigger and associated particle momenta, the double peak is present/absent for out of plane/in plane trigger particle direction.

The difference in path lengths traveled by partons in the medium is at the core of the idea that the away side structures may include contributions of $2 \rightarrow 3$ processes. For instance, when the hard scattering resulting in this kind of processes happens close to the edge, there is a large chance that at least one of the three final state partons travels a large distance through the medium therefore, having a high probability of being absorbed. The resulting hadronic process has two particles in the final state but its origin is an underlying partonic event with three partons in the final state, one of which was unable to hadronize. Conservation of momentum at the parton level followed by collinear fragmentation gives rise to a distinctive angular dependence in the azimuthal correlation whereby, the angular difference between leading and away side particles is close to $2\pi/3$ radians, regardless of whether one or two partons in the away side survive their passing through the medium and are able to hadronize.

The above scenario has been put forward and explored in Refs. [5], using the leading order QCD matrix elements for $2 \rightarrow 3$ parton processes. A serious limitation of this approach stems from the way the collinear singularities are avoided. This was implemented by restricting the phase space for parton production to the regions where

the angular difference between leading and away side partons is far from 0 and π . To overcome such limitation, in this work we present a Monte Carlo approach to study azimuthal correlations in $p + p$ and $A + A$ collisions. We use the MadGraph5 [6] event generator, which includes built-in functions to cancel collinear and soft divergences for $2 \rightarrow 3$ parton processes. To study medium effects we use the modified fragmentation function approach. We also study $2 \rightarrow 3$ parton processes that contribute to only two hadrons in the final state. The work is organized as follows: In Sec. II we present the basics of the description for three hadron production in $p + p$ and $A + A$ collisions. In Sec. III we introduce a Monte Carlo event generator to implement the calculation of azimuthal angular correlations. To study the details of the effect of energy loss on partons within different momentum bins, in Sec. IV we present both the parton and hadron p_T distributions for the Monte Carlo generated events. We note that for the model parameters used, low p_T hadrons come from relatively high p_T partons. We use these samples to build the azimuthal angular correlations in Sec. V. Finally, we discuss our results and conclude in Sec. VI, in particular we argue that the double peak/broadening in the away side observed in data may still be described within this approach, by considering the interaction of those partons that are not able to hadronize outside the medium, but still interact with the bulk partons.

II. THREE-HADRON PRODUCTION

In previous works [5] we have computed the differential cross section for three-hadron production in $p + p$

and $A + A$ collisions at mid-rapidity. In order to show the essentials of that approach, we hereby summarize it and refer the reader to the aforementioned references for further details.

In the case of $p + p$ collisions the differential cross section was obtained by convoluting over the incoming momentum fraction, the initial distributions f_p for partons within the colliding protons, the matrix elements $|\mathcal{M}_{2 \rightarrow 3}|^2$ and the fragmentation functions $D_{P/H}$. For this we used the CTEQ6 parametrization [7], the leading order matrix elements describing the process at the parton level [8] and KKP fragmentation functions [9], for a given total center of mass energy \sqrt{s} available for the collision. We considered collinear fragmentation thus, the angles that define the direction of the away-side hadrons, θ_i^H ($i = 2, 3$), are linearly related to the the parton angles θ_j ($j = 2, 3$).

To consider the process within a central heavy-ion collision and thus account for the effects of energy loss, we resorted to the model put forward in Ref. [10]. The model considers an initial gluon density obtained from the overlap of two colliding nuclei, each with a Woods-Saxon density profile. The gluon density of the medium is diluted only due to longitudinal expansion of the plasma since transverse expansion is neglected.

The gluon density ρ_g is related to the nuclear geometry of the produced medium. We use the modified fragmentation functions [10]

$$\tilde{D}_{P_n/H_m}(z_{nm}) = \left(1 - e^{-\langle L/\lambda \rangle}\right) \left[\frac{z'_{nm}}{z_{nm}} D_{P_n/H_m}(z'_{nm}) + \langle L/\lambda \rangle \frac{z'_{nm;g}}{z_{nm}} D_{P_n/H_m}(z'_{nm;g}) \right] + e^{-\langle L/\lambda \rangle} D_{P_n/H_m}(z_{nm}), \quad (1)$$

where $z'_{nm} = h_m/(p_n - \Delta E_n)$ is the rescaled momentum fraction, of hadron H_m originated from the fragmenting parton P_n , $z'_{nm;g} = \langle L/\lambda \rangle (h_m/\Delta E_n)$ is the rescaled momentum fraction of the radiated gluon, ΔE_n is the average radiative parton energy loss and $\langle L/\lambda \rangle$ is the average number of scatterings. Both ΔE_n and $\langle L/\lambda \rangle$ are related to the gluon density of the produced medium. This relation comes in by considering the path length traveled through the medium by the partons produced in the hard scattering. The path length is determined from the radial position r and the angle ϕ that the leading parton makes with the radial direction, within the medium.

The average energy loss ΔE_n is also proportional to the one dimensional energy loss $\langle dE_n/dL \rangle_{1d}$ parametrized as

$$\left\langle \frac{dE_n}{dL} \right\rangle_{1d} = \epsilon_0 \left[\frac{p_n}{\mu_0} - 1.6 \right]^{1.2} \left[7.5 + \frac{p_n}{\mu_0} \right]^{-1}. \quad (2)$$

The one-dimensional energy loss per unit length parameter, ϵ_0 , is related to the mean free path λ_0 by $\epsilon_0 \lambda_0 = 0.5$ GeV. Notice that Eq. (2) means that there is a lower threshold for p_n given by $p_n^{\text{thresh}} = 1.6 \times \mu_0 = 2.4$ GeV below which the one-dimensional energy loss becomes meaningless. This is interpreted as reflecting the fact that the energy loss model cannot produce hadrons by fragmentation for partons below this momentum threshold. Those partons should thus be absorbed by the medium and their effect has to be accounted for by other hadronization mechanisms.

The above described procedure has an inherent limitation which we have already identified in Refs. [5]. These are related to the angular cuts required to avoid the collinear singularities when two of the final state hadrons are either parallel or antiparallel. In order to overcome

such limitations we proceed to present a Monte Carlo implementation of two and three hadron production in $p + p$ and $A + A$ environments dedicated to the study of azimuthal angular correlations.

III. MONTE CARLO EVENT GENERATOR WITH ENERGY LOSS

A. Parton level event generator

We implement the production of parton events using MadGraph5 [6], in $p + p$ collisions at RHIC energies at mid-rapidity ($|\eta| < 0.5$). MadGraph5 generates the helicity amplitude subroutines to build the hard scattering matrix elements, used as inputs for the partonic event generator. It also generates a set of functions, inspired by the dipole subtraction method [11], that remove the soft and collinear singularities in the phase-space integrated matrix elements arising under certain kinematical conditions, producing an unweighted set of hard scattering partonic events. A typical run involves declaring the values for certain parameters such as the beam energy, the factorization scale μ^2 , the fragmentation scale Q^2 , the p_T bin size of the final state partons and the value of parameters like `xqcut` that controls the numerical cancellation of the singularities, according to the particular kinematics. It is worth mentioning that, as suggested in the literature [6], we use values for `xqcut` below 10 GeV.

B. Hadron level event generator

In order to achieve hadron events we take the parton level events and evolve the partons into hadrons with collinear fragmentation.

To study $p + p$ collisions, partons are fragmented into hadrons, by means of KKP fragmentation [9]. To describe medium effects on the propagation of partons and their hadronization in a nuclear collision, we include energy loss effects through KKP modified fragmentation functions [10]. In the former case, parton i with momentum p is assigned a random value of momentum fraction z , which allows it to evolve into hadron H with momentum p^H . In the latter, we take into account that the hard scattering can take place anywhere within the nuclear collision overlap area and that the produced partons can travel in any direction. This is implemented by assigning the hard scattering a random radial position r and a random direction ϕ that the leading parton makes with the outward radial direction. These parameters are used to determine the average number of scatterings $\langle L/\lambda \rangle$, the energy loss ΔE_i for each parton and their modified momentum fractions z'_i . In this way the hadron level events are characterized by the particle species and their kinematical variables both in $p+p$ and $A+A$ collisions. Notice that the KKP fragmentation functions are valid only for hadron momentum fractions z in the range $0.1 < z < 0.8$

which affects the shape of the azimuthal correlations for the away-side hadrons' relative angular separation close to 0 and π radians.

For the nuclear environment, since the minimum allowed parton momentum for hadronization is, according to the model in Ref. [10], $p_T = 2.4$ GeV, then we have three different types of events corresponding to the number of partons that are absorbed by the medium due to energy loss. Notice that this implies that there is a contribution from $2 \rightarrow 3$ partonic processes (where one of the final state parton is absorbed by the medium) to the di-hadron azimuthal correlation function.

IV. p_T DISTRIBUTIONS FOR $2 \rightarrow \{2, 3\}$ HADRON PRODUCTION

In order to better characterize parton energy loss, we first build the p_T distributions for partons produced in given momentum bins. We then build the hadron p_T distributions that these partons originate and identify the corresponding momentum bins where these hadrons are produced. For the sake of definiteness, we carry out this procedure for exclusive momentum bins $2 - 4$, $6 - 8$, $10 - 12$ and $14 - 16$ GeV.

Figure 1 shows the parton and hadron p_T distributions at central rapidity $|\eta| \leq 0.5$ for $2 \rightarrow 2$ events, both in $p + p$ ($\epsilon_0 = 0$) and $A + A$ ($\epsilon_0 = 2$ GeV/fm) collisions at $\sqrt{s_{NN}} = 200$ GeV. On the left (right) column we show the leading (away) hadron p_T distribution. The leading hadron has been defined, event by event, as the hadron with the largest p_T , thus for each parton p_T bin, the away hadron momentum distribution is shifted towards lower values of p_T when compared to the leading one. The effect is more pronounced in $A + A$ collisions due to energy loss. Notice also that momentum conservation at the parton level is reflected by the fact that the parton momentum distribution is the same for leading and away side hadrons.

Figure 2 shows the parton and hadron p_T distributions for $2 \rightarrow 3$ events, both in $p + p$ ($\epsilon_0 = 0$) and in $A + A$ ($\epsilon_0 = 2$ GeV/fm) collisions. In the figure, the left column shows the momentum distribution of the leading hadron which, as before is the hadron with the largest p_T in the event, the middle column displays the away side hadron selected as the hadron with the second largest momentum and the right column shows the away side hadron with the lowest p_T in the event. It is also interesting to note that the bulk of the hadron events with low momenta (in the range $0.2 \text{ GeV} \leq p_T \leq 2 \text{ GeV}$), come from parton events with momenta in the range $2 \text{ GeV} \leq p_T \leq 10 \text{ GeV}$, whereas the hadron events with higher momenta (in the range $2 \text{ GeV} \leq p_T \leq 4 \text{ GeV}$), come from parton events with momenta in the range $10 \text{ GeV} \leq p_T \leq 16 \text{ GeV}$.

We now focus on the characterization of the events that contribute to the di-hadron azimuthal correlation either from $2 \rightarrow 2$ or from $2 \rightarrow 3$ parton processes. Figure 3

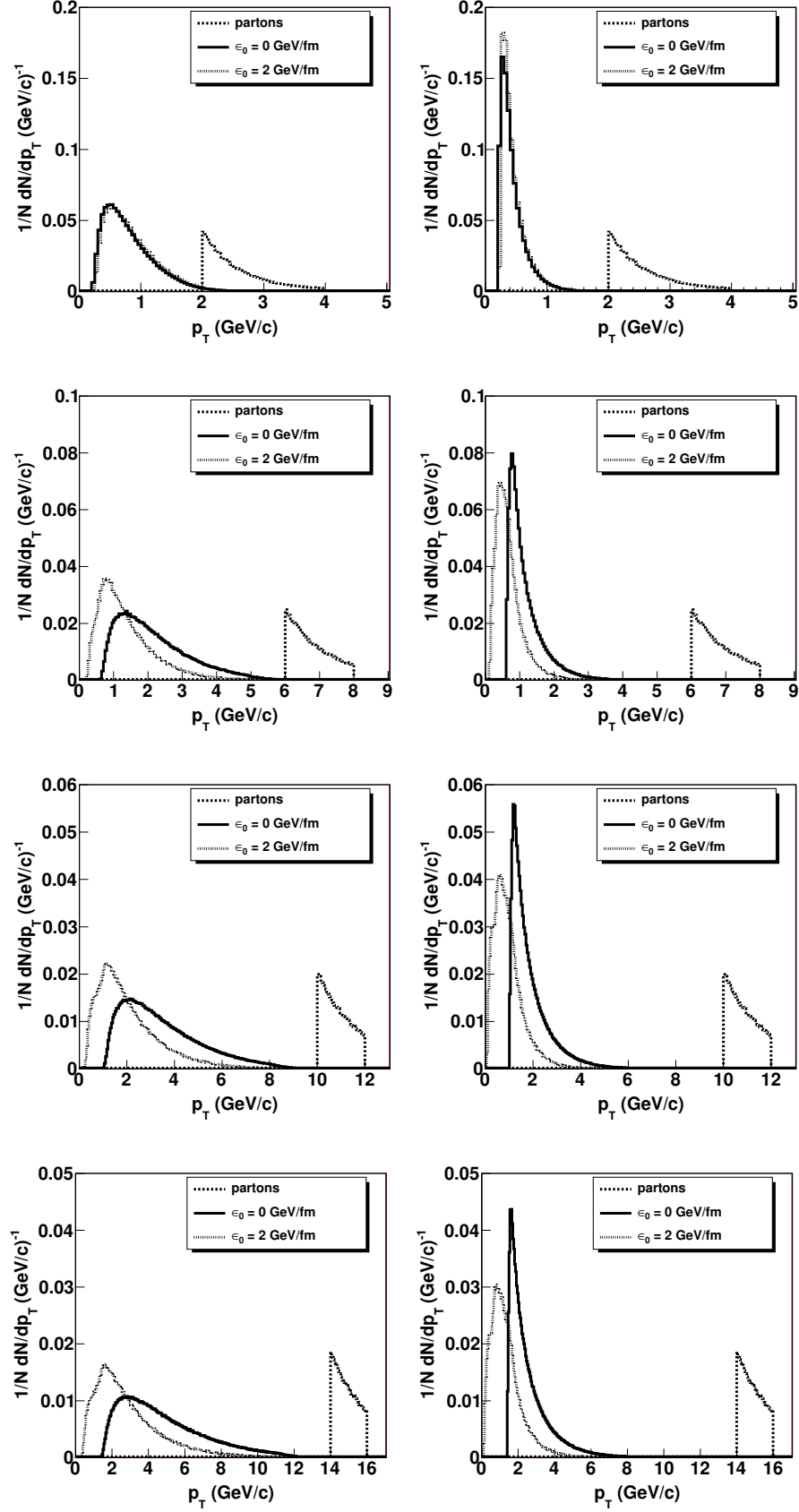


FIG. 1: Parton (dotted lines) and hadron p_T distributions for $2 \rightarrow 2$ events in $p + p$ ($\epsilon_0 = 0$, solid lines) and in $A + A$ ($\epsilon_0 = 2 \text{ GeV/fm}$, dash-dotted lines) collisions for central rapidity $|\eta| \leq 0.5$ at $\sqrt{s_{NN}} = 200 \text{ GeV}$. On the left/right column we show the p_T distribution for the leading/away hadron. The hadrons come from partons produced in four different momentum bins, from top to bottom: 2 – 4, 6 – 8, 10 – 12 and 14 – 16 GeV.

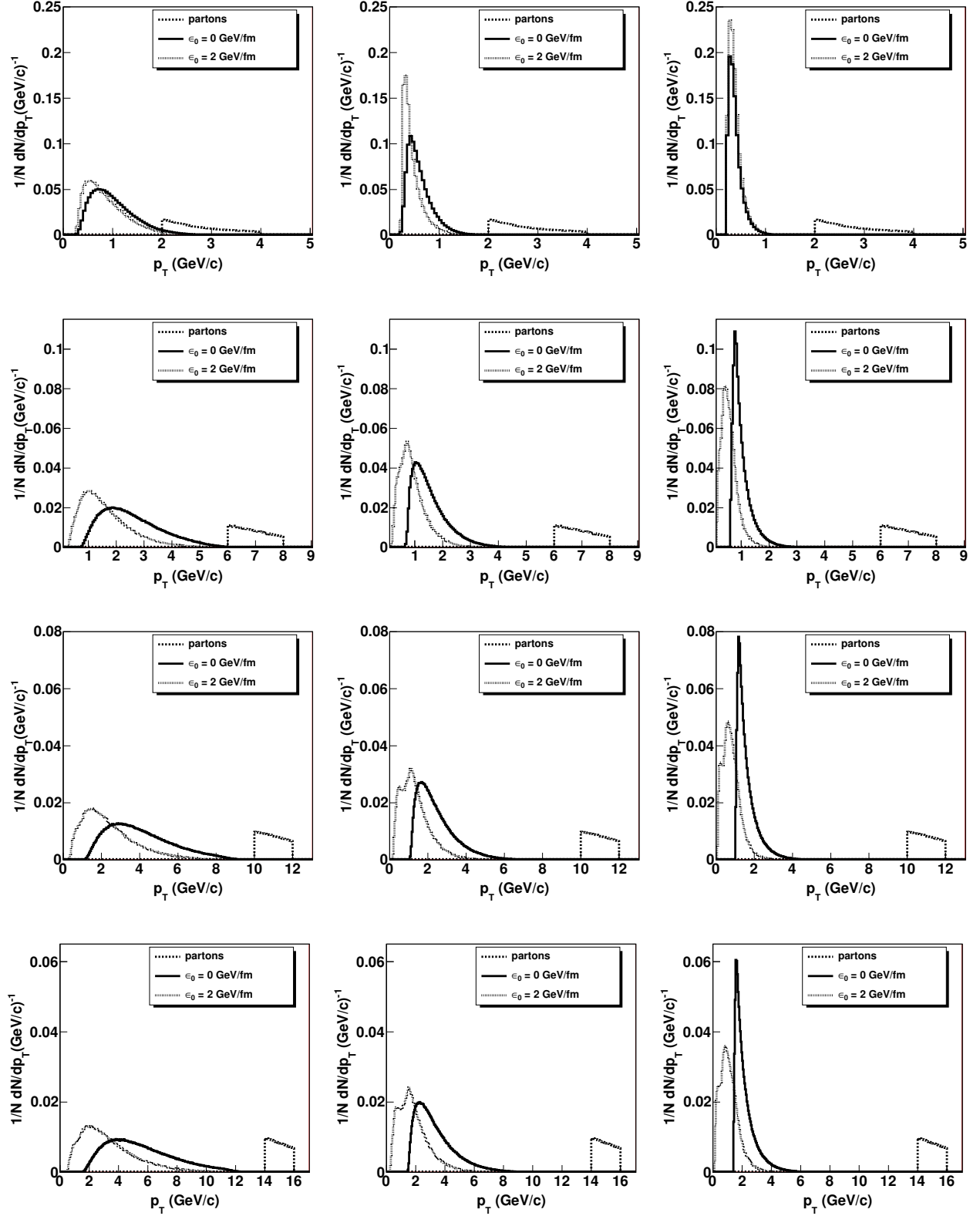


FIG. 2: Parton (dotted lines) and hadron p_T distributions for 2 \rightarrow 3 events in $p+p$ ($\epsilon_0 = 0$, solid lines) and in $A+A$ ($\epsilon_0 = 2$ GeV/fm, dash-dotted lines) collisions for central rapidity $|\eta| \leq 0.5$ at $\sqrt{s_{NN}} = 200$ GeV. From left to right we show the p_T distributions for the leading and the away hadrons, which come from partons produced in four different momentum bins, from top to bottom: 2 – 4, 6 – 8, 10 – 12 and 14 – 16 GeV.

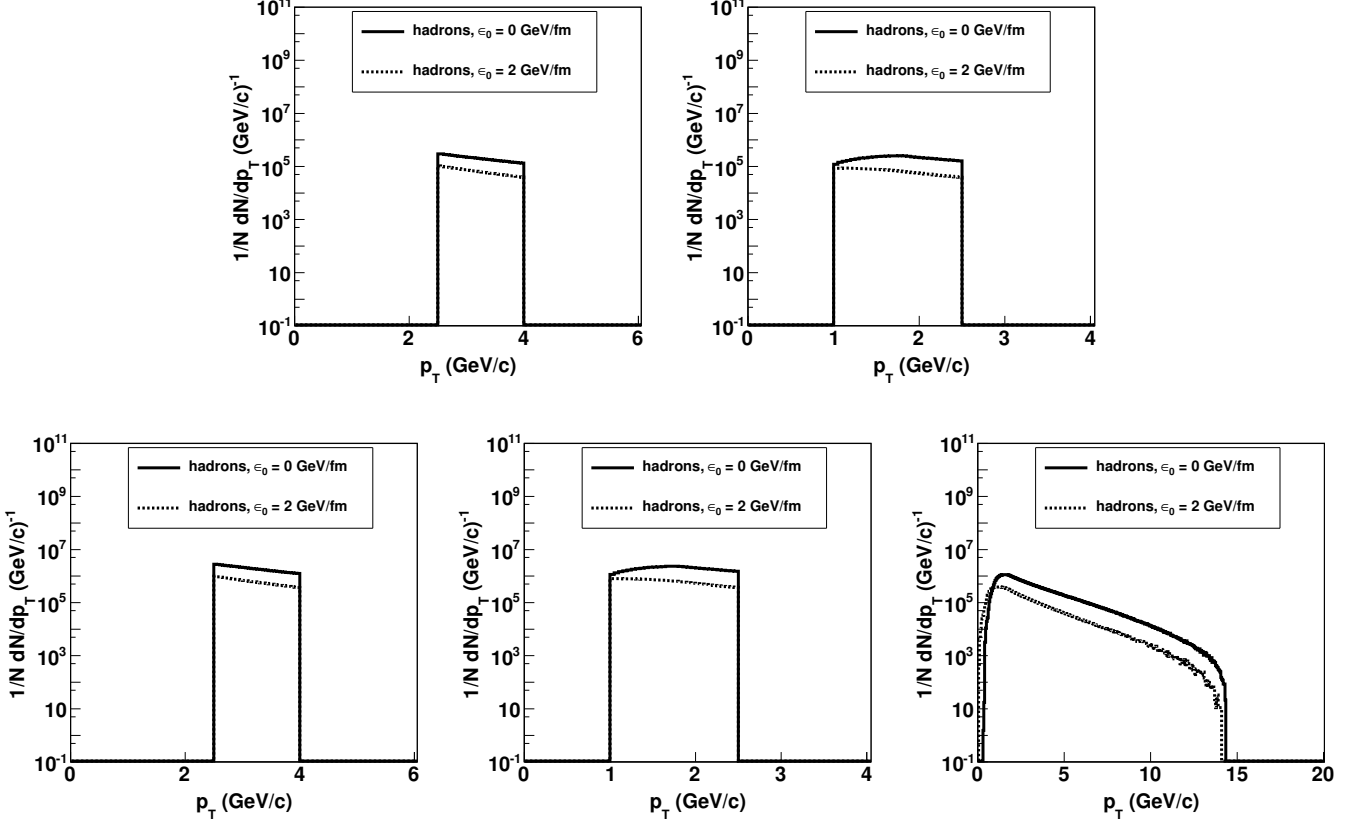


FIG. 3: Hadron p_T distributions for events that contribute to the di-hadron azimuthal correlation. Shown are $2 \rightarrow 2$ (upper row) and $2 \rightarrow 3$ (lower row) processes. The solid lines correspond to the case without medium and the dotted lines to the case within the medium. In both cases the leading hadron is in the momentum bin $2.5 \text{ GeV} \leq p_T \leq 4 \text{ GeV}$. For the upper row the away side hadron is in the momentum bin $1 \text{ GeV} \leq p_T \leq 2.5 \text{ GeV}$ whereas in the second row, at least one of the away side hadrons is in the momentum bin $1 \text{ GeV} \leq p_T \leq 2.5 \text{ GeV}$.

shows the hadron p_T distribution calculated under the aforementioned kinematical conditions, where we use all the parton exclusive momentum bins, 2 GeV wide, in the range 2 – 18 GeV. The leading hadron is in the bin $2.5 \text{ GeV} \leq p_T \leq 4 \text{ GeV}$. In the first row we show $2 \rightarrow 2$ events where the away side hadron is in the momentum bin $1 \text{ GeV} \leq p_T \leq 2.5 \text{ GeV}$ and in the second row we show $2 \rightarrow 3$ events where at least one of the away side hadrons is in the momentum bin $1 \text{ GeV} \leq p_T \leq 2.5 \text{ GeV}$. We choose these hadron momentum bins to compare with the analysis of Ref. [12]. Also, the selection of hadron events from parton p_T bins in specified ranges favors mercedes-like configurations for hadrons. Notice that as expected, in each case the distributions without medium are consistently higher than the ones with medium effects.

V. THREE-HADRON AZIMUTHAL CORRELATIONS

We now look at the azimuthal correlations for the away side considering the contributions from $2 \rightarrow 2$ and $2 \rightarrow 3$ hadron events.

Figure 4 shows the di-hadron azimuthal angular correlation normalized to the number of parton events and to the bin size from $2 \rightarrow 2$ (upper row) and $2 \rightarrow 3$ (lower row) events. For this figure we use parton p_T bins 2 – 4 and 10 – 12 GeV for $p + p$ ($\epsilon_0 = 0$) and $A + A$ ($\epsilon_0 = 2 \text{ GeV/fm}$) collisions at $\sqrt{s_{NN}} = 200 \text{ GeV}$. Notice the typical peak shape at π radians in the $2 \rightarrow 2$ case, that in our approach arises due to collinear fragmentation, whereas in the $2 \rightarrow 3$ case the peaks are located at $2\pi/3$ and $4\pi/3$ radians and have a finite width. In the 2 – 4 GeV parton p_T bin, there is a marked difference between the height of the peaks for hadrons produced in the $p + p$ and $A + A$ cases. This is due to the fact that in the medium, the model considers a threshold at $p_T^{\text{thresh}} = 2.4 \text{ GeV}$ below which the parton is unable to

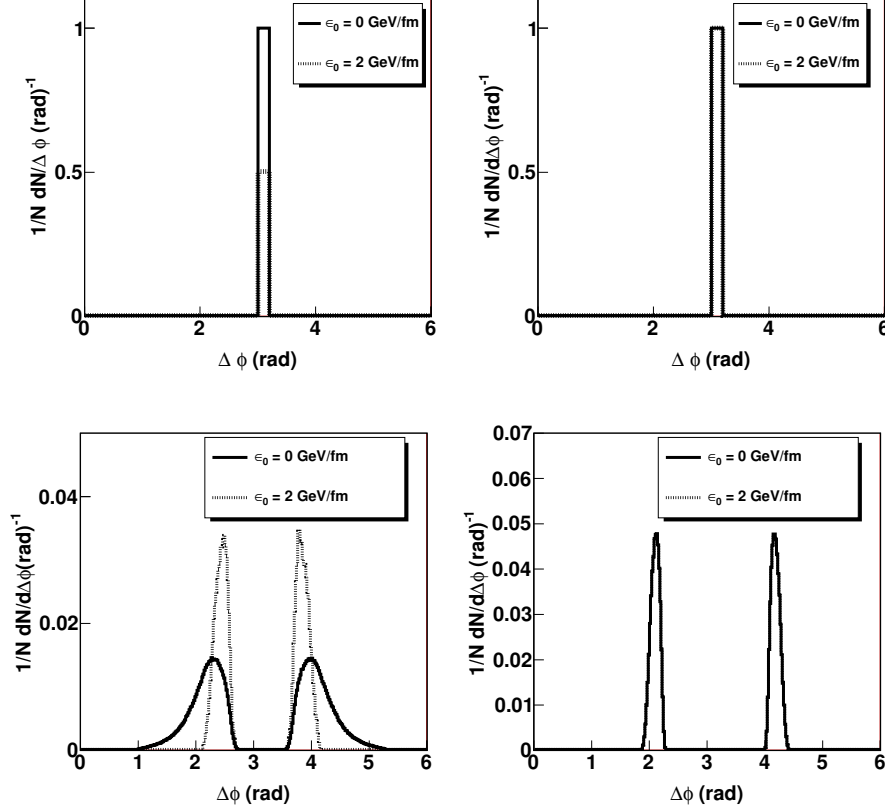


FIG. 4: Di-hadron azimuthal angular correlation normalized to the number of parton events and to the bin size from $2 \rightarrow 2$ (upper row) and $2 \rightarrow 3$ (lower row) events in parton p_T bins $2-4$ and $10-12$ GeV for $p+p$ ($\epsilon_0 = 0$) and $A+A$ ($\epsilon_0 = 2$ GeV/fm) collisions

hadronize and this value lies within the considered p_T bin. For all parton p_T bins higher than this one, the correlation of hadrons produced in both cases coincide, since the threshold value p_T^{thresh} is outside such bin. This is illustrated with the $10-12$ GeV parton p_T bin on the right column of Fig. 4.

Finally, to extract information from the three-hadron azimuthal correlation function in a two dimensional analysis, one possibility is to look at this function in terms of the angular difference $\Delta\phi = \theta_3^H - \theta_2^H$ of the away side hadrons for a range of angles of one of the away side hadrons, say, θ_2^H . Figure 5 shows this correlation in the proton and nuclear environments with $\sqrt{s_{NN}} = 200$ GeV for a leading hadron momentum $2.5 \text{ GeV} \leq p_T \leq 4$ GeV and away side hadron momenta $1 \text{ GeV} \leq p_T \leq 2.5$ GeV, integrated over angular range $1.65 \text{ radians} \leq \theta_2^H \leq 2.2$ radians. Shown are the normalized histograms for $\epsilon_0 = 2$ GeV/fm (solid line) and $\epsilon_0 = 0$ (squares) obtained from the present Monte Carlo approach and from the approach in Refs. [5] with $\epsilon_0 = 2$ GeV/fm (dotted line), compared to preliminary data from the PHENIX Collaboration [12]. Notice that the Monte Carlo approach histogram has a more defined peak at $\Delta\phi = 2.2$ radians, than the approach where we regulated the divergences

with angular cuts. The difference between the Monte Carlo result and the data, can be understood by recalling that we have implemented collinear fragmentation. To be able to populate the regions for $\Delta\phi \lesssim 1$ radians and $\Delta\phi \gtrsim 2.5$ radians, we would need to consider the contribution of the leading hadron and go beyond collinear fragmentation.

VI. SUMMARY AND CONCLUSIONS

In this work we have presented a Monte Carlo approach to compute di-hadron correlation functions including contributions from $2 \rightarrow 2$ and $2 \rightarrow 3$ parton processes in $p+p$ and $A+A$ collisions. The production of parton events in $p+p$ is implemented using MadGraph5 where hadron events are obtained by evolving the partons into hadrons with collinear fragmentation by means of KKP fragmentation. For the nuclear environment we follow a modified fragmentation function approach whereby the hard scattering is assigned a random radial position r and a random direction ϕ that the leading parton makes with the outward radial direction. These parameters are used to determine the average number of scatterings, the

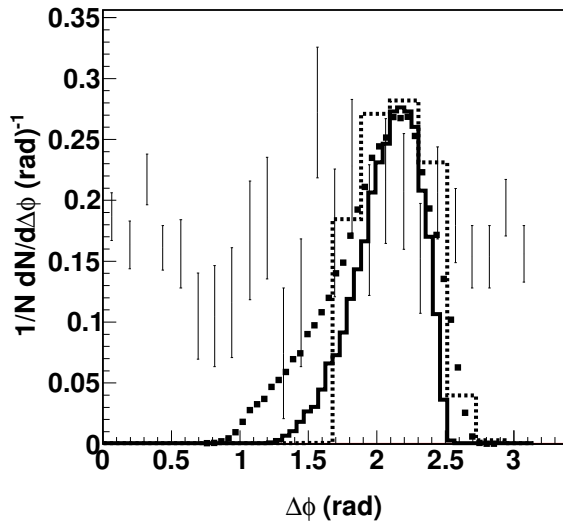


FIG. 5: Normalized di-hadron correlation in the nuclear environment with $\epsilon_0 = 2$ GeV/fm as a function of the angular difference $\Delta\phi = \theta_3^H - \theta_2^H$, integrated over angular range 1.65 radians $\leq \theta_2^H \leq 2.2$ radians for a leading hadron momentum $2.5 \text{ GeV} \leq p_T \leq 4 \text{ GeV}$ and away side hadron momenta $1 \text{ GeV} \leq p_T \leq 2.5 \text{ GeV}$. The solid line and the squares correspond to the Monte Carlo approach with $\epsilon_0 = 2 \text{ GeV/fm}$ and $\epsilon_0 = 0$, respectively, and the dotted line to the approach in Refs. [5] with $\epsilon_0 = 2 \text{ GeV/fm}$. Data are from the PHENIX Collaboration [12].

energy loss for each parton and their modified momentum fractions. We use the Monte Carlo approach to overcome the limitations set by collinear and soft divergences that otherwise have to be handled by means of angular cuts. We have studied the hadron p_T ranges that are populated when partons fragment. To be fully quantitative, one requires to generate Monte Carlo samples covering a wide range of parton p_T , both for $2 \rightarrow 2$ and $2 \rightarrow 3$ processes.

Our approach on the other hand, based on populating hadron p_T bins from given parton p_T bins although reducing the need of a large Monte Carlo sample still has limitations, in particular, to assess quantitatively the relative contributions between $2 \rightarrow 2$ and $2 \rightarrow 3$ processes. Work to overcome this limitation is underway and will be reported elsewhere.

We conclude that since the energy loss model considers a threshold parton momentum $p_T^{\text{thresh}} = 2.4 \text{ GeV}$ below which partons cannot fragment, there is a need to study the way those partons interact with the bulk medium and that do not hadronize through fragmentation. These partons are rather abundant, since the low momentum part of their spectrum is more populated, and thus their effect must be considered. When these partons are produced in $2 \rightarrow 3$ processes, due to momentum conservation they still come out from the hard scattering mainly with the characteristic mercedes-like configuration. Their interaction with the bulk partons should produce a transfer of momentum along these directions that will deform the medium producing showers of low momentum hadrons bearing the same distinctive angular distance of the original partons. This avenue is currently being pursued and the results will also be reported elsewhere.

Acknowledgments

Support for this work has been received in part from DGAPA-UNAM under grant number PAPIIT-IN103811, CONACyT-México under grant number 128534, *Programa de Intercambio UNAM-UNISON*, the DOE Office of Nuclear Physics through Grant No. DE-FG02-09ER41620, the “Lab Directed Research and Development” grant LDRD 10-043 (Brookhaven National Laboratory), and by The City University of New York through the PSC-CUNY Research Award Program, grant 63404-0042. J.J.-M. would like to thank A. Dumitru for discussions on this topic.

-
- [1] C. Adler *et al.* (STAR Collaboration), Phys. Rev. Lett. **90** 082302 (2003); A. Adare *et al.* (PHENIX Collaboration), Phys. Rev. C **78**, 014901 (2008).
 - [2] M. M. Aggarwal, *et al.* (STAR Collaboration), Phys. Rev. C **82**, 024912 (2010); A. Adare, *et al.* (PHENIX Collaboration), Phys. Rev. Lett. **104**, 252301 (2010).
 - [3] P. Sorensen (STAR Collaboration), J. Phys. G **38**, 124029 (2011). K. Aamodt *et al.* (ALICE Collaboration), Phys. Rev. Lett. **107**, 032301 (2011).
 - [4] F. Wang (STAR Collaboration), arXiv:1201.5006; H. Agakishiev *et al.* (STAR Collaboration), arXiv:1010.0690.
 - [5] A. Ayala, J. Jalilian-Marian, J. Magnin, A. Ortiz, G. Paic and M. E. Tejeda-Yeomans, Phys. Rev. Lett. **104**, 042301 (2010); Phys. Rev. C **84**, 024915 (2011).
 - [6] J. Alwall *et al.*, JHEP **0709**, 28 (2007); R. Frederix, T. Gehrmann and N. Greiner, JHEP **0809**, 122 (2008); JHEP **1006**, 86 (2010).
 - [7] H. L. Lai, J. Huston, Z. Li, P. Nadolsky, J. Pumplin, D. Stump and C.P. Yuan, Phys. Rev. D **82**, 054021 (2010).
 - [8] R.K. Ellis and J.C. Sexton, Nucl. Phys. B **269**, 445 (1986).
 - [9] B.A. Kniehl, G. Kreimer and B. Potter, Nucl. Phys. B **582**, 514 (2000).
 - [10] H. Zhang, J.F. Owens, E. Wang and X.-N. Wang, Phys. Rev. Lett. **98**, 212301 (2007).
 - [11] S. Catani and M.H. Seymour, Nucl. Phys. B **485**, 291 (1997); Z. Kunszt and D.E. Soper, Phys. Rev. D **46**, 192 (1992).
 - [12] N. N. Ajitanand (PHENIX Collaboration), Indian J. Phys. **84**, 1647 (2010).